

NMF vs. ICA for Light Source Separation under AC Illumination

Ruri Oya, Ryo Matsuoka and Takahiro Okabe

Department of Artificial Intelligence, Kyushu Institute of Technology, Japan
okabe@ai.kyutech.ac.jp

Keywords: Light Source Separation, Alternating Current, Flicker, NMF, ICA.

Abstract: Artificial light sources powered by an electric grid change their intensities in response to the grid's alternating current (AC). Their flickers are usually too fast to notice with our naked eyes, but can be captured by using cameras with short exposure time settings. In this paper, we propose a method for light source separation under AC illumination on the basis of Blind Source Separation (BSS). Specifically, we show that light source separation results in matrix factorization, since the input images of a scene illuminated by multiple AC light sources are represented by the linear combinations of the basis images, each of which is the image of the scene illuminated by only one of the light sources, with the coefficients, each of which is the intensity of the light source. Then, we make use of Non-negative Matrix Factorization (NMF), because both the pixel values of the basis images and the intensities of the light sources are non-negative. We experimentally confirmed that our method using NMF works better than Independent Component Analysis (ICA), and studied the performance of our method under various conditions: varying exposure times and noise levels.

1 INTRODUCTION

Artificial light sources in our surroundings are often powered by an electric grid, and therefore their intensities rapidly change in response to the grid's alternating current (AC). Their flickers are usually too fast to notice with our naked eyes, but can be captured by using cameras with short exposure time settings (Vollmer and Möllmann, 2015). Such rapid flickers could make auto white balance unnatural (Hsu et al., 2008).

Sheinin *et al.* (Sheinin et al., 2017) propose a method for light source separation under AC illumination. Their proposed method decomposes an image sequence of a scene illuminated by multiple AC light sources into the images of the scene, each of which is illuminated by only one of the light sources, and the temporal intensity profiles of the light sources. They make use of their self-build coded-exposure camera synchronized to AC and the dataset of temporal intensity profiles of various light sources, and then achieve light source separation even for dark scenes such as a city-scale scene at night. Later, Sheinin *et al.* (Sheinin et al., 2018) achieve light source separation under AC illumination by using consumer rolling-shutter cameras, but still require the dataset of temporal intensity profiles of various light sources.

In this paper, we propose a method for light source separation under AC illumination on the basis of

Blind Source Separation (BSS). Specifically, we show that light source separation results in matrix factorization, since the input images are represented by the linear combinations of the basis images, each of which is the image of the scene illuminated by only one of the light sources, with the coefficients, each of which is the intensity of the light source. Then, we make use of Non-negative Matrix Factorization (NMF) (Berry et al., 2007) for BSS, because both the pixel values of the basis images and the intensities of the light sources are non-negative.

We conducted a number of experiments and confirmed that our proposed method using NMF works better than Independent Component Analysis (ICA) (Hyvärinen and Oja, 2000). In addition, we studied the performance of our method, which is based on fast flickers of light sources' intensities, under various conditions: varying exposure times and noise levels.

Our proposed method based on BSS does not require the dataset of light sources' temporal intensity profiles nor the self-build camera synchronized to AC in contrast to Sheinin *et al.* (Sheinin et al., 2017; Sheinin et al., 2018). Therefore, our method is applicable to image sequences captured by using consumer cameras and applicable to unknown light sources that are not included in the dataset, although it is not suited for dark scenes because the images captured by using those cameras have low S/N ratios in general.

The main contributions of this study are twofold. First, we propose a method for light source separation under AC illumination on the basis of BSS; it does not require the dataset of light sources' temporal intensity profiles nor the self-build camera synchronized to AC. Second, we experimentally confirmed that NMF works better than ICA for light source separation under AC illumination, and studied the behavior of our proposed method using NMF under varying exposure times and noise levels.

2 PROPOSED METHOD

According to the superposition principle of light, an image of a scene taken under multiple light sources is represented by a convex combination of the *basis images*, each of which is the image taken under one of the light sources. Specifically, the pixel value i_{pcf} of an input image sequence at the p -th pixel ($p = 1, 2, 3, \dots, P$) in the c -th channel ($c = 1, 2, 3$) and in the f -th frame ($f = 1, 2, 3, \dots, F$) is represented as

$$i_{pcf} = \sum_{n=1}^N b_{pcn} a_{nf}. \quad (1)$$

Here, N is the number of light sources, b_{pcn} is the pixel value of the n -th basis image at the p -th pixel and in the c -th channel, and a_{nf} is the intensity of the n -th light source in the f -th frame.

We can rewrite eq.(1) in a matrix form as

$$\mathbf{I} = \mathbf{BA}, \quad (2)$$

where \mathbf{I} is the $3P \times F$ matrix consisting of the pixel values of the input image sequence, \mathbf{B} is the $3P \times N$ matrix consisting of the pixel values of the N basis images, and \mathbf{A} is the $N \times F$ matrix consisting of the intensities of the N light sources. Therefore, light source separation results in the problem of matrix factorization; factorizing the matrix \mathbf{I} of the input image sequence into the matrix \mathbf{B} of the basis images and the matrix \mathbf{A} of the light sources' intensities.

The necessary condition for light source separation is that the number of equations is larger than or equal to the number of unknowns: $(3P \times F) \geq (3P \times N + N \times F)$. When the number of pixel P is large enough compared to the number of light sources N , light source separation is possible if $F > N$. Our proposed method makes use of NMF (Berry et al., 2007) for matrix factorization, because both the pixel values of the basis images and the intensities of the light sources are non-negative. Specifically, our method estimates the matrices \mathbf{B} and \mathbf{A} by the minimization;

$$\min_{\{\mathbf{B}, \mathbf{A}\}} \frac{1}{2} \|\mathbf{I} - \mathbf{BA}\|_{\text{Fr}}^2 \quad (3)$$



Figure 1: The first three images of the synthetic image sequences of (a) Scene 1, (b) Scene 2, and (c) Scene 3.

subject to the conditions that all the elements of the matrices \mathbf{B} and \mathbf{A} are non-negative. Here, $\|\cdot\|_{\text{Fr}}$ stands for the Frobenius norm of a matrix.

Since the matrix \mathbf{I} is represented by the product of the matrices \mathbf{B} and \mathbf{A} , there are the ambiguities in scale and order between those matrices. In addition, since $\mathbf{BA} = \mathbf{BU}^{-1}\mathbf{UA}$, the ambiguity represented by the $N \times N$ regular matrix \mathbf{U} , that keeps all the elements of the matrices \mathbf{BU}^{-1} and \mathbf{UA} non-negative, could occur.

3 EXPERIMENTS

To confirm the effectiveness of our proposed method, we conducted qualitative and quantitative evaluation by using both synthetic and real images.

3.1 NMF vs. ICA

We compared the following three methods for light source separation under AC illumination.

- **NMF** (our proposed method) decomposes the input images into the basis images and the light sources' intensities according to eq.(3).
- **ICA-1** decomposes the input images into the basis images and the light sources' intensities so that the basis images are independent of each other.
- **ICA-2** decomposes the input images into the basis images and the light sources' intensities so that the light sources' intensities are independent of each other.

In our implementation, we used the alternating least squares algorithm (Berry et al., 2007) for NMF, and FastICA (Hyvärinen and Oja, 2000) for ICA-1 and ICA-2.

Table 1: The PSNRs of the basis images estimated by using NMF, ICA-1, and ICA-2 for Scenes 1, 2, and 3. The numerical values in each cell are the PSNRs for the first/second basis images.

method\scene	1	2	3
NMF	52.52/42.22	44.70/53.72	30.97/24.46
ICA-1	17.57/31.06	39.16/20.53	24.39/33.28
ICA-2	23.32/42.20	27.46/46.27	23.38/ 37.40

Table 2: The RMSEs of the intensity profiles of the light sources estimated by using NMF, ICA-1, and ICA-2 for Scenes 1, 2, and 3. The numerical values in each cell are the RMSEs for the first/second light sources.

method\scene	1	2	3
NMF	0.001/0.003	0.001/0.004	0.012/0.014
ICA-1	0.023/0.045	0.017/0.017	0.010/0.014
ICA-2	0.036/0.012	0.036/0.012	0.034/ 0.001

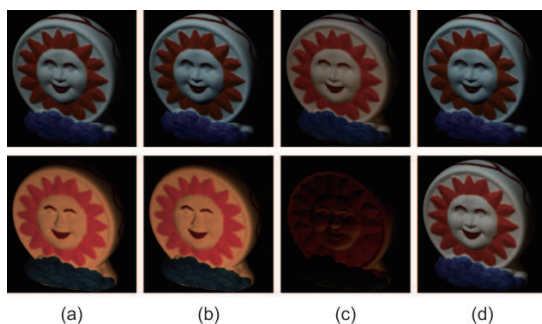


Figure 2: The results of light source separation for Scene 1: (a) the ground truth of the basis images, and the basis images estimated by using (b) NMF, (c) ICA-1, and (d) ICA-2.

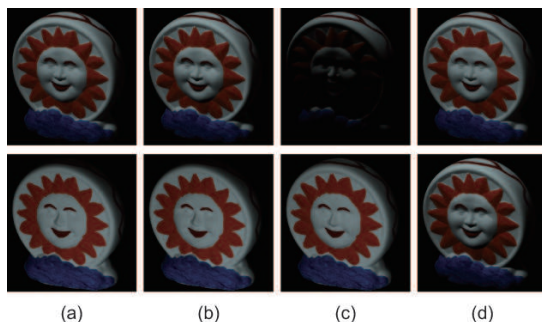


Figure 3: The results of light source separation for Scene 2: (a) the ground truth of the basis images, and the basis images estimated by using (b) NMF, (c) ICA-1, and (d) ICA-2.

Synthetic Images:

We synthesized three input image sequences by using the two datasets; one is for basis images under varying light source directions (Barron and Malik, 2015) and the other is for light sources' temporal intensity profiles sampled at 26 points per cycle (Sheinin et al., 2017). We tested three illumination conditions; a scene is illuminated by two light sources with different colors and from different directions (Scene 1), those with the same color and from different directions (Scene 2), and those with different colors and

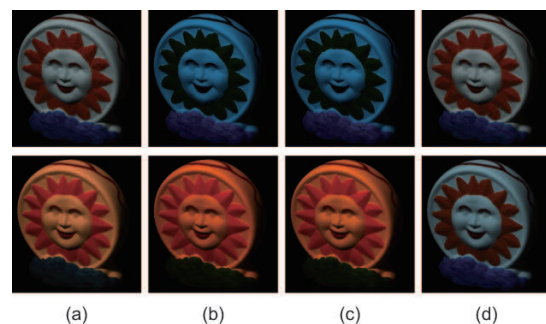


Figure 4: The results of light source separation for Scene 3: (a) the ground truth of the basis images, and the basis images estimated by using (b) NMF, (c) ICA-1, and (d) ICA-2.

from the same direction (Scene 3) as shown in Figure 1.

Figures 2, 3, and 4 show the results of light source separation for Scenes 1, 2, and 3 respectively: (a) the ground truth of the basis images, and the basis images estimated by using (b) NMF, (c) ICA-1, and (d) ICA-2. Tables 1 and 2 summarize the PSNRs of the estimated basis images and the RMSEs of the estimated intensity profiles of the light sources for those scenes by using NMF, ICA-1, and ICA-2 respectively.

We can see that NMF works well and that its performance is better than those of ICA-1 and ICA-2, when both the colors and directions of the light sources are different (Scene 1) and when only the directions of the light sources are different (Scene 2). On the other hand, all the methods do not necessarily work well when the directions of the light sources are the same (Scene 3). This is because there are shadows in Scenes 1 and 2. Specifically, since the directions of the light sources are different in Scenes 1 and 2, there are some areas that are illuminated by only one of the light sources. Because we can directly observe the flickers due to the single light source there, those shadows could be important clues for light source separation.

Table 3: The PSNRs of the basis images estimated by using NMF, ICA-1, and ICA-2 for Scenes 4, 5, and 6. The numerical values in each cell are the PSNRs for the first/second basis images.

method \ scene	4	5	6
NMF	31.34/30.44	32.56/31.97	29.72/30.88
ICA-1	23.11/20.47	31.72/25.95	21.39/18.98
ICA-2	26.13/21.31	19.52/25.74	15.61/26.10

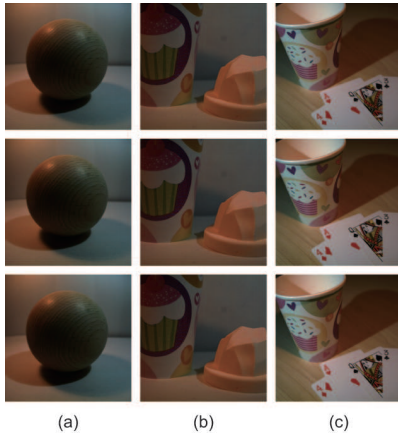


Figure 5: The first three images of the real image sequence of (a) Scene 4, (b) Scene 5, and (c) Scene 6.

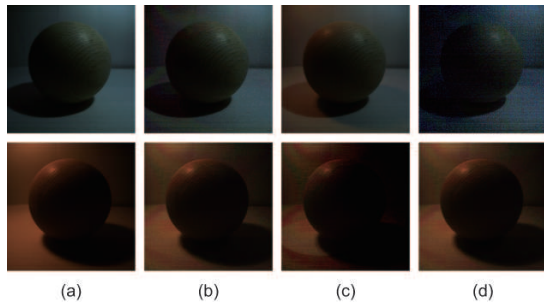


Figure 6: The results of light source separation for Scene 4: (a) the ground truth of the basis images, and the basis images estimated by using (b) NMF, (c) ICA-1, and (d) ICA-2.

Real Images:

We captured the image sequences of three scenes, *i.e.* Scenes 4, 5, and 6, each of which is illuminated by two light sources powered by an electric grid with 60 Hz as shown in Figure 5. We used the high-speed camera FASTCAM Mini UX50 from Photolon with the frame rate of 2,500 fps/1,000 fps and with the exposure time of 0.4 ms/1 ms for Scenes 4 and 5/Scene 6 respectively.

Figures 6, 7, and 8 show the results of light source separation for those scenes: (a) the ground truth of the basis images, and the basis images estimated by using (b) NMF, (c) ICA-1, and (d) ICA-2. We consider the images captured when turning only one of the light sources on as the ground truth of the basis images. Table 3 summarizes the PSNRs of the basis images

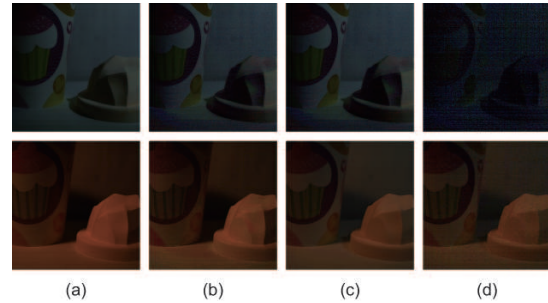


Figure 7: The results of light source separation for Scene 5: (a) the ground truth of the basis images, and the basis images estimated by using (b) NMF, (c) ICA-1, and (d) ICA-2.

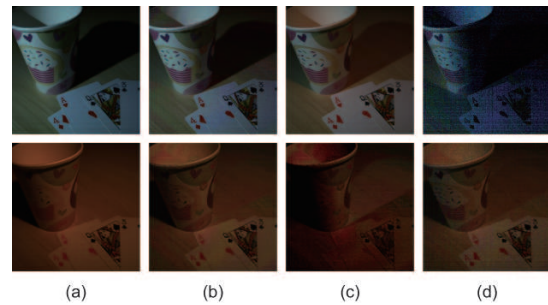


Figure 8: The results of light source separation for Scene 6: (a) the ground truth of the basis images, and the basis images estimated by using (b) NMF, (c) ICA-1, and (d) ICA-2.

estimated by using NMF, ICA-1, and ICA-2.

We obtained the results consistent to those using synthetic images. Figure 6, 7, and 8 qualitatively show that NMF works better than ICA-1 and ICA-2. In particular, the colors and shadows in the basis images estimated by using ICA-1 are often inaccurate, and the basis images estimated by using ICA-2 are often darker than the ground truth due to negative pixel values¹. Table 3 quantitatively shows that NMF works better than ICA-1 and ICA-2 significantly.

3.2 Sensitivity Analysis

The performance of our proposed method using NMF depends on exposure times as well as image noises, since light source separation under AC illumination

¹Since the scales of the basis images estimated by using NMF and ICA are ambiguous, we adjusted the scales of the estimated basis images so that the PSNRs are maximized for fair quantitative evaluation

Table 4: The PSNRs of the basis images estimated by using NMF for varying standard deviations of Gaussian noises and varying exposure times. The numerical values in each cell are the PSNRs for the first/second basis images.

	0.25 ms	0.5 ms	1 ms	2 ms	4 ms	8 ms
$\sigma=0$	50.03/34.89	50.02/34.88	50.01/34.83	49.90/34.62	49.29/33.87	43.21/32.44
$\sigma=1$	46.22/35.07	46.19/35.06	46.05/35.02	45.58/34.86	43.91/34.19	40.02/32.58
$\sigma=2$	42.13/34.46	42.11/34.47	42.08/34.41	41.86/34.30	41.24/33.80	39.80/32.54
$\sigma=4$	41.08/33.49	41.08/33.48	41.03/33.46	40.89/33.37	40.57/33.03	39.43/32.21
$\sigma=8$	39.89/31.78	39.85/31.87	39.83/31.74	39.76/31.59	39.36/31.89	38.22/31.13

Table 5: The RMSEs of the intensity profiles of the light sources estimated by using NMF for varying standard deviations of Gaussian noises and varying exposure times. The numerical values in each cell are the RMSEs for the first/second light sources.

	0.25 ms	0.5 ms	1 ms	2 ms	4 ms	8 ms
$\sigma=0$	0.003/0.000	0.003/0.000	0.003/0.000	0.004/0.000	0.006/0.000	0.023/0.000
$\sigma=1$	0.002/0.002	0.002/0.002	0.002/0.002	0.002/0.002	0.004/0.003	0.013/0.010
$\sigma=2$	0.003/0.008	0.003/0.008	0.003/0.008	0.003/0.008	0.005/0.010	0.011/0.012
$\sigma=4$	0.003/0.012	0.004/0.012	0.003/0.012	0.004/0.012	0.006/0.012	0.011/0.013
$\sigma=8$	0.007/0.013	0.009/0.015	0.008/0.015	0.006/0.014	0.015/0.013	0.013/0.015

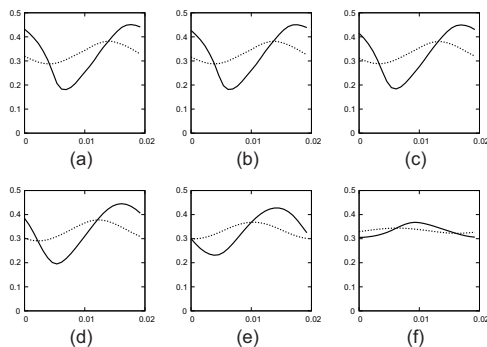


Figure 9: The intensity profiles of the first (solid lines) and second (dotted lines) light sources when the exposure times are (a) 0.25 ms, (b) 0.5 ms, (c) 1 ms, (d) 2 ms, (e) 4 ms, and (f) 8 ms respectively.

makes use of fast flickers of light sources' intensities. Accordingly, we studied the sensitivity of our method using NMF to exposure times and noises by using synthetic images.

Specifically, we interpolated the temporal intensity profiles (Sheinin et al., 2017), which are sampled at 26 points per cycle, by spline interpolation, and computed the intensity profiles with the exposure times from 0.25 ms to 8 ms. Then, we synthesized the images with varying exposure times by combining the basis images for Scene 1 with those light sources' intensities, and added zero-mean Gaussian noises, whose standard deviation σ is from 1 to 8 for 8-bit pixel values, to them.

Tables 4 and 5 summarize the PSNRs of the basis images and the RMSEs of the intensity profiles of the light sources estimated by using NMF. We can see that the PSNRs of the basis images are getting

worse as not only the standard deviation of the Gaussian noises but also the exposure time increase. This is because the intensity profiles of the light sources are getting smoother and the flickers also becomes invisible as the exposure time increases as shown in Figure 9.

4 CONCLUSION

In this paper, we proposed a method for light source separation under AC illumination on the basis of BSS; we decompose the image sequence of a scene illuminated by multiple AC light sources into the basis images and the light sources' intensities. Specifically, we show that light source separation results in matrix factorization, and make use of NMF for BSS because both the pixel values of the basis images and the intensities of the light sources are non-negative. We experimentally confirmed that our method using NMF works better than ICA, and studied the performance of our method under various conditions: varying exposure times and noise levels. Our future work includes light source separation under more than two light sources, the improved separation by taking noise removal into consideration, and the application of the separation results.

ACKNOWLEDGMENTS

This work was partially supported by JSPS KAKENHI Grant Numbers JP18H05011 and JP17H01766.

REFERENCES

- Barron, J. and Malik, J. (2015). Shape, illumination, and reflectance from shading. *IEEE TPAMI*, 38(7):1670–1687.
- Berry, M., Browne, M., Langville, A., Pauca, V., and Plemmons, R. (2007). Algorithms and applications for approximate nonnegative matrix factorization. *Computational Statistics & Data Analysis*, 52(1):155–173.
- Hsu, E., Mertens, T., Paris, S., Avidan, S., and Durand, F. (2008). Light mixture estimation for spatially varying white balance. *ACM TOG*, 27(3):1–7.
- Hyvärinen, A. and Oja, E. (2000). Independent component analysis: algorithms and applications. *Neural Networks*, 13(4–5):411–430.
- Sheinin, M., Schechner, Y., and Kutulakos, K. (2017). Computational imaging on the electric grid. In *Proc. IEEE CVPR2017*, pages 6437–6446.
- Sheinin, M., Schechner, Y., and Kutulakos, K. (2018). Rolling shutter imaging on the electric grid. In *Proc. IEEE ICCP2018*, pages 1–12.
- Vollmer, M. and Möllmann, K.-P. (2015). Flickering lamps. *European Journal of Physics*, 36(035027).